

Compact 4 × 4 Butler matrix with Non-Standard Phase Differences for IoT Applications

A. Bekasiewicz and S. Koziel

Butler matrices represent a popular class of feeding networks for antenna arrays. Large dimensions and the lack of flexibility in terms of achievable output phase difference make conventional Butler structures of limited use for modern communication devices. In this work, a compact planar 4 × 4 matrix with non-standard relative phase shifts of -30° , 150° , -120° , and 60° has been proposed. The structure is designed to operate at the centre frequency of 2.45 GHz. Small dimensions of 31.3 mm × 22.9 mm make it useful for Internet of Things applications. The structure operates from 2.35 GHz to 2.55 GHz which covers the industrial, scientific and medical (ISM) bandwidth. At the centre frequency, the measured amplitude and phase imbalance are 1.65 dB and $\pm 4.3^\circ$, respectively. The proposed circuit has been compared to the state-of-the-art structures from the literature.

Introduction: Feeding networks are the key components of antenna arrays. A type of thereof, Butler matrices (BMs), are characterized by the ability to provide different phase shifts between the outputs, depending on the excited input port. A conventional planar BM is composed of branch line couplers (BLCs), phase shifters, and crossovers [1]. In a 4 × 4 configuration, it can produce progressive phase differences of $\pm 45^\circ$ or $\pm 135^\circ$ at the outputs. Due to lack of phase-related flexibility, as well as large dimensions applicability of conventional BMs to modern communication devices, including Internet of Things (IoT) systems operating within the ISM band is limited.

Design of miniaturized BMs has recently gained attention of the research community [2]-[7]. Popular size reduction techniques include replacement of the BM building blocks by their compact counterparts [3], [4], implementation of the structures on multi-layer substrates [5], or development of BMs without some of the components [6], [7]. Application of the mentioned techniques allows for obtaining between 60% to 85% miniaturization. Despite a significant size reduction compared to conventional structures [4], [6], [7], large physical dimensions of these BMs are still a limiting factor for their application in small-size devices.

BMs characterized by non-standard relative phase differences between the output ports are normally constructed using components that support arbitrary phase-shifts [8], [9]. In [8], the control over the output phases is maintained using phase shifters with the unequal electrical lengths. Another method, where unconventional BLCs are used to control the Butler matrix phase differences, has been discussed in [9]. Both approaches proved to be useful for increasing the BM functionality over the conventional structures.

In this work, a compact planar 4 × 4 Butler matrix with non-standard relative phase differences between output ports of -30° , 150° , -120° , and 60° , is proposed. The structure comprises two pairs of hybrid BLCs with the phase shifts of 75° and 60° , respectively. Dimensions and footprint of the optimized BM are 31.3 mm × 22.9 mm and 717 mm², respectively. The size reduction has been achieved using a combination of folded BLC structures, and compact crossovers involving the microstrip-to-coplanar-waveguide transition. The centre frequency of the proposed circuit is 2.45 GHz, and it operates within 2.35 GHz to 2.55 GHz bandwidth. The magnitude and phase-difference imbalances of the BM at the centre frequency are 1.65 dB and $\pm 4.3^\circ$, respectively. Small dimensions and high performance make the proposed structure suitable for applications in small-form-factor IoT devices. The presented BM has been benchmarked against state-of-the-art circuits from the literature, and validated experimentally.

Design Concept: Conceptual illustration of the proposed Butler matrix is shown in Fig. 1. The structure is constituted by two pairs of BLCs with phase differences of β_1 and β_2 , respectively, two phase shifters β_3 , as well as two crossovers introducing the phase shift of β_c .

The presented BM can provide relative phase differences of $\Delta\theta_i$ ($i = 1, \dots, 4$, corresponds to the port P_i used for structure excitation) between the outputs P_{5-8} that exceed the capabilities of conventional

structures. The electrical properties of the BM components (see Fig. 1) required to obtain the desired $\Delta\theta_i$, can be determined from [9]

$$\beta_1 = 0.5\beta_2 - 0.25\pi \quad (1)$$

$$\beta_2 = 2\Delta\theta_1 \quad (2)$$

$$\beta_3 = -0.25\pi \quad (3)$$

Note that $\Delta\theta_2 = \Delta\theta_1 + \pi$, $\Delta\theta_3 = 0.5\beta_2 - 0.5\pi$, and $\Delta\theta_4 = \Delta\theta_3 + \pi$ [9]. Consequently, $\Delta\theta_{2-4}$ depend on $\Delta\theta_1$ from (1)-(3). For demonstration, the phase differences of the BM considered here are set to $\Delta\theta_{1-4} = \{-30^\circ, 150^\circ, -120^\circ, 60^\circ\}$ that are obtained using $\beta_1 = -75^\circ$, $\beta_2 = -60^\circ$, and $\beta_3 = -45^\circ$, respectively.

A conceptual illustration of the BLC structure that can realize phase differences β_1 and β_2 is shown in Fig. 2a. The k th coupler ($k = 1, 2$) consists of two equal-length sections with the normalized characteristic impedance of $z_{1,k}$, and the electrical length of $\varphi_{1,k} = -90^\circ$, as well as two sections with impedance $z_{2,k}$ and the lengths of $\varphi_{2,k}$, and $\varphi_{3,k}$, respectively. The electrical parameters the BLCs can be found by solving [10], [11]:

$$z_{1,k} = \sqrt{\frac{z_{2,k}^2}{1 - z_{2,k}^2}} \quad (4)$$

$$z_{2,k} = \frac{\tan(\beta_k)(\tan^2(0.5\varphi_{2,k}) - 1)}{2 \tan(0.5\varphi_{2,k})} \quad (5)$$

$$\varphi_{3,k} = 2 \tan^{-1} \left(\sqrt{\frac{1}{\tan(0.5\varphi_{2,k})}} \right) \quad (6)$$

The values determined from (4)-(6) required to obtain selected $\Delta\theta_{1-4}$ are $Z_{1,1} = 44.65 \Omega$, $Z_{2,1} = 32.16 \Omega$, $\varphi_{2,1} = 100.56^\circ$, $\varphi_{3,1} = 79.44^\circ$, $Z_{1,2} = 42.59 \Omega$, $Z_{2,2} = 32.2 \Omega$, $\varphi_{2,2} = 110.71^\circ$, and $\varphi_{3,2} = 69.30^\circ$ (note that $Z_{1-2,k} = Z_0 z_{1-2,k}$). The calculated electrical parameters are used as a starting point for the design of the BM components.

Butler matrix components: The compact BLC structure incorporated into the proposed Butler matrix is shown in Fig. 2b. The circuit and the entire BM are implemented on a dielectric substrate with $\epsilon_r = 3.74$, $h = 0.168$ mm, and $\tan\delta = 0.0037$. The couplers are miniaturized by means of folding the conventional transmission line sections. The vector of geometry parameters that represent the k th BLC is $\mathbf{x}_k = [w_{1,k} w_{2,k} c_{1,k} c_{2,k} l_{1,k} l_{2,k} l_{3,k}]^T$. The relative variables are $r_{1,k} = 3w_{2,k} + 3c_{2,k} - w_{1,k}$, $r_{2,k} = l_{2,k} + w_{2,k} + c_{2,k}$, and $r_{3,k} = l_{3,k} + w_{2,k} + c_{1,k}$, whereas $w_0 = 0.35$ to ensure 50 Ω input impedance (cf. Fig. 1). The unit for all design parameters is mm. The dimensions of BLC₁ and BLC₂ have been obtained through local numerical optimization (gradient algorithm) oriented towards maintaining the reflection and isolation of each coupler below -20 dB within 2.35 GHz to 2.55 GHz range. Other requirements involved minimization of the power split imbalance and maintaining the desired phase differences β_1 , β_2 at the centre frequency of $f_0 = 2.45$ GHz [2], [11]. The starting points for BLCs design $\mathbf{x}_1^{(0)} = [0.34 \ 0.55 \ 0.3 \ 0.3 \ 2.2 \ 1.6]^T$ and $\mathbf{x}_2^{(0)} = [0.46 \ 0.6 \ 0.3 \ 0.3 \ 2 \ 2.3 \ 1.3]^T$ are determined through recalculation of the electrical parameters (see the previous section) to the microstrip line dimensions. The optimized designs are $\mathbf{x}_1^* = [0.36 \ 0.56 \ 0.32 \ 0.39 \ 2.94 \ 2.18 \ 1.44]^T$ and $\mathbf{x}_2^* = [0.38 \ 0.56 \ 0.2 \ 0.4 \ 3.23 \ 2.58 \ 1.13]^T$. The optimized BLC₁ and BLC₂ are only 8.55 mm × 6.77 mm = 57.85 mm² and 8.23 mm × 6.9 mm = 56.8 mm², respectively. The obtained circuits exhibit 80% and 79.5% miniaturization w.r.t. their conventional counterparts.

Small dimensions of crossovers are ensured by replacing the cascade-based circuits by a simple microstrip-to-coplanar-waveguide transition [12]. The geometry of the used circuit is shown in Fig. 3. Its design parameters $\mathbf{x}_c = [w_1 \ w_2 \ w_3 \ l_1 \ l_2 \ l_3 \ s_1 \ s_2 \ d_1 \ d_2 \ r]^T$ have been adjusted to maximize isolation between the intersected transmission lines, as well as to maintain their equal electrical length. The tuned design $\mathbf{x}_c^* = [0.5 \ 0.7 \ 0.5 \ 4.22 \ 0.78 \ 3.55 \ 0.2 \ 0.2 \ 0.6 \ 0.2 \ 0.3]^T$ provides in-band reflection and isolation both below -30 dB, as well as equal phase shift of $\beta_c = 61.4^\circ$ (cf. Fig. 1). The structure size is 6.05 mm × 6.05 mm = 36.6 mm².

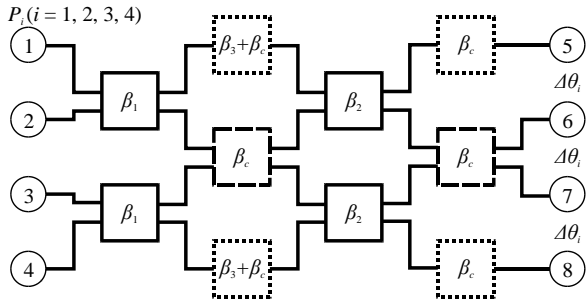


Fig. 1 Butler matrix – conceptual illustration. Solid, dashed, and dotted boxes represent BLCs, crossovers, and phase shifters, respectively.

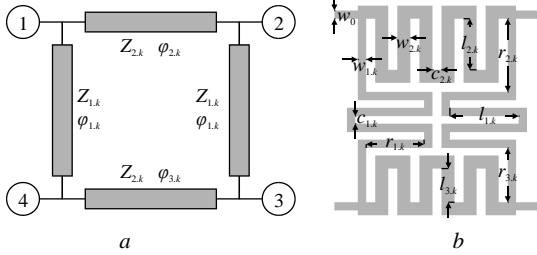


Fig. 2 Branch line coupler with arbitrary phase difference.
a Conceptual illustration of the structure
b Geometry of the miniaturized circuit

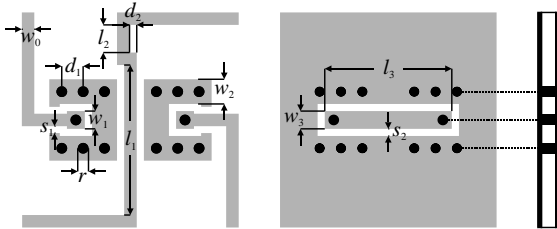


Fig. 3 Compact crossover with microstrip-to-coplanar-waveguide transition. From left: top, bottom, and cross-section view. Black circles represent vias.

The proposed BM incorporates the phase shifters in the form of simple, folded transmission lines. The lengths of the meandered lines can be adjusted individually in order to provide enhanced control over the relative phase differences between P_5 to P_8 ports. The vector of phase shifters lengths is $\mathbf{x}_p = [p_1 p_2 p_3 p_4]^T$ (cf. Fig. 4a). Its initial values $\mathbf{x}_p^{(0)} = [4.0 \ 4.0 \ 1.8 \ 1.8]^T$ are calculated from β_3 and β_c .

Numerical results and measurements: Geometry of the proposed Butler matrix is shown in Fig. 4a. The vector structure adjustable variables is $\mathbf{x}_b = [x_1 x_2 p_1 p_2 p_3 p_4]^T$. The initial design is $\mathbf{x}_b^{(0)} = [0.36 \ 0.56 \ 0.32 \ 0.39 \ 2.94 \ 2.18 \ 1.44 \ 0.38 \ 0.56 \ 0.2 \ 0.4 \ 3.23 \ 2.58 \ 1.13 \ 4.0 \ 4.0 \ 1.8 \ 1.8]^T$. The final design $\mathbf{x}_b^* = [0.36 \ 0.56 \ 0.32 \ 0.39 \ 2.94 \ 2.19 \ 1.45 \ 0.39 \ 0.58 \ 0.22 \ 0.45 \ 3.34 \ 2.56 \ 1.13 \ 3.76 \ 3.6 \ 1.33 \ 1.42]^T$ is obtained as a result of BM fine tuning oriented towards reduction of the phase-difference and magnitude errors. The size of the optimized structure, expressed as $A \times B$ (see Fig. 4), is only $31.3 \text{ mm} \times 22.9 \text{ mm} = 716.8 \text{ mm}^2$. The EM simulation results show that, in the 2.35 GHz to 2.55 GHz band, the BM offers reflection below -13 dB , but also the amplitude and phase imbalance below 0.6 dB and slightly above $\pm 5^\circ$, whereas at the centre frequency the figures are below 0.55 dB and $\pm 4.1^\circ$, respectively.

The proposed BM has been fabricated (see Fig. 4b) and measured. A comparison of simulation and measurement results is shown in Fig. 5, whereas the performance figures of the structure, i.e., in-band reflection (R_{BW}) and isolation (I_{BW}), as well as magnitude (ΔM) and phase-shift (ΔP) imbalance within the frequency band and at f_0 are gathered in Table 1. The overall agreement between the simulation and the measured results is acceptable having in mind that the magnitude is expressed in dB. The discrepancies between the responses mostly result from the fabrication tolerances, as well as the errors introduced by the manual circuit assembly, and imperfections of the measurement setup.

Comparison with benchmark structures: The proposed circuit has been compared against BMs from the literature in terms of the size, and performance (EM simulation results). The considered figures include bandwidth (defined for isolation and reflection both below -15 dB), magnitude imbalance, and phase-shift error (both at the centre frequency) [2], [4]-[6], [9]. The dimensions of all structures are expressed in the guided wavelength λ_g calculated for a given centre frequency, and the electrical parameters of the substrate used for circuit implementation. The results from Table 2 indicate that the proposed BM provides competitive performance and outperforms the benchmark circuits in terms of the size.

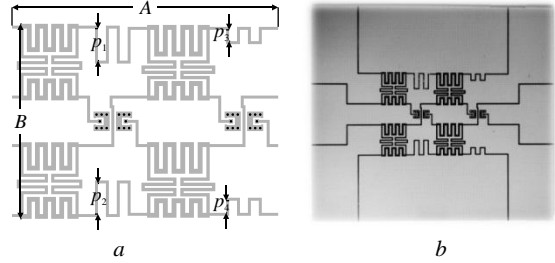


Fig. 4 Compact Butler matrix with non-standard phase differences
a Optimized design with highlight on phase shifters dimensions
b Photograph of the manufactured structure prototype

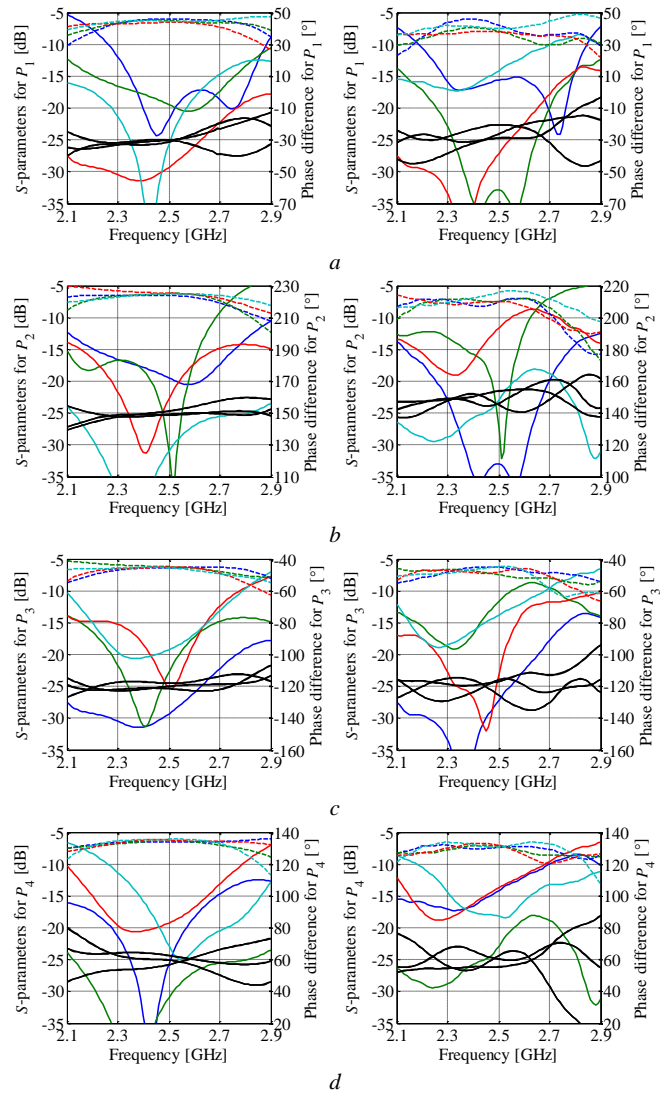


Fig. 5 BM: comparison of simulations (left) and measurements (right) w.r.t. reflection/isolation (solid colour), transmission (dashed colour) and phase-shift (black) responses for the structure excited through:
a Port P_1 (phase difference at the output ports: -30°)
b Port P_2 (phase difference at the output ports: 150°)
c Port P_3 (phase difference at the output ports: -120°)
d Port P_4 (phase difference at the output ports: 60°)

Table 1: Compact BM: comparison of simulations and measurements.

Excitation	Port P_1		Port P_2		Port P_3		Port P_4	
	Sim.	Meas.	Sim.	Meas.	Sim.	Meas.	Sim.	Meas.
R_{BW} [dB]	-15.4	-15.3	-16.9	-14.4	-16.4	-16.7	-13.3	-16.6
I_{BW} [dB]	-17.2	-12.9	-17.2	-10.0	-18.2	-10.0	-18.3	-12.7
ΔM_{BW} [dB]	0.55	2.09	0.60	1.81	0.51	1.62	0.43	0.98
ΔM_{f_0} [dB]	0.55	1.65	0.40	1.66	0.23	1.01	0.38	0.79
ΔP_{BW} [°]	± 2.1	± 7.3	± 2.5	± 6.6	± 2.8	± 8.4	± 5.3	± 7.5
ΔP_{f_0} [°]	± 1.4	± 4.3	± 0.9	± 4.0	± 1.7	± 1.0	± 4.1	± 3.5

Table 2: Proposed BM: benchmark against the state-of-the-art circuits.

	Performance figures				Size	
	f_0 [GHz]	BW [%]	ΔM_{f_0} [dB]	ΔP_{f_0} [°]	Dimensions [mm × mm]	Dimensions [$\lambda_g \times \lambda_g$]
[9]	5.8	7.3	0.45	± 6.0	71.4×119	1.89×3.15
[2]	1.0	N/A	1.20	± 1.0	87.8×82.4	0.49×0.46
[6]	6.0	7.2	0.4	± 0.9	58.9×57.9	1.96×1.93
[4]	1.8	5.5	2.40	± 5.9	99.5×127	0.82×1.04
[5]	28	3.2	4.70	± 16	16.8×14.9	N/A
This work	2.45	9.4	0.55	± 4.1	31.3×22.9	0.44×0.32

Conclusion: In this work, a compact 4×4 Butler matrix for IoT applications has been presented. The structure provides a non-standard relative phase shifts between output ports of -30° , 150° , -120° , 60° , respectively. Circuit's electrical dimensions are $0.44\lambda_g \times 0.32\lambda_g$ mm, with overall footprint of only 720 mm^2 . The small size has been achieved using folded couplers and miniaturized crossovers. Simulation results indicate that the proposed BM offers reflection below -13 dB within the frequency range from 2.35 GHz to 2.55 GHz. Furthermore, at 2.45 GHz measured magnitude and phase errors of the BM are below 1.7 dB and $\pm 4.5^\circ$, respectively. The structure outperforms state-of-the-art circuits in terms of size while maintaining competitive performance.

Acknowledgments: This work was supported in part by National Centre for Research and Development Grant NOR/POLNOR/HAPADS/0049/2019-00, by National Science Centre of Poland Grant 2017/27/B/ST7/00563, and by Icelandic Centre for Research (RANNIS) Grant 206606051.

A. Bekasiewicz, and S. Koziel (Faculty of Electronics, Telecommunications and Informatics, Gdansk University of Technology, Narutowicza 11/12, 80-233 Gdansk, Poland)

E-mail: bekasiewicz@ru.is

S. Koziel: also with Department of Engineering, Reykjavik University, Menntavegur 1, 101 Reykjavik, Iceland

References

1. Milligan, T.A. 'Modern Antenna Design' (John Wiley & Sons, New York, 2005).
2. Koziel, S., Kurgan, P.: 'Low-cost optimization of compact branch-line couplers and its application to miniaturized Butler matrix design,' European Microwave Conf., Rome, 2014, pp. 227-230.
3. Letavin, D.A., Shabunin, S.N.: 'Construction of a 4x4 Butler microstrip matrix with reduced dimensions', Ural Symp. Biomed. Eng., Radioelectronics Inf. Tech., Yekaterinburg, 2020, pp. 257-260.
4. Xu, H.-X., Wang, G.-M., Wang, X.: 'Compact Butler matrix using composite right/left handed transmission line,' *Electronics Lett.*, 2011, **47**, (19), pp. 1081-1083.

5. Kim, S., Yoon, S., Lee, Y., Shin, H.: 'A miniaturized Butler matrix based switched beamforming antenna system in a two-layer hybrid stackup substrate for 5G applications', *Electronics*, 2019, **8**, (11), pp. 1-11.
6. Tian, G., Yang, J., Wu, W.: 'A novel compact Butler matrix without phase shifter', *IEEE Microwave Wireless Comp. Lett.*, 2014, **24**, (5), pp. 306-308.
7. Bhowmik, P., Moyra, T.: 'Modelling and validation of a compact planar Butler matrix by removing crossover', *Wireless Pers. Comm.*, 2017, **95**, pp. 5121-5132.
8. Tajik, A., Shafiei Alavijeh, A., Fakharzadeh, M.: 'Asymmetrical 4×4 Butler matrix and its application for single layer 8×8 Butler matrix,' *IEEE Trans. Ant. Prop.*, 2019, **67**, (8), pp. 5372-5379.
9. Ren, H., Arigong, B., Zhou, M., Ding J., Zhang, H.: 'A novel design of 4×4 Butler matrix with relatively flexible phase differences,' *IEEE Ant. Wireless Prop. Lett.*, 2016, **15**, pp. 1277-1280.
10. Wong, Y.S., Zheng, S.Y., Chan, W.S.: 'Quasi-arbitrary phase-difference hybrid coupler', *IEEE Trans. Microwave Theory Tech.*, 2012, **60**, (6), pp. 1530-1539.
11. Nocedal, J., Wright, S.: 'Numerical Optimization', (Springer, New York, 2006).
12. Tajik, A., Fakharzadeh, M., Mehrany, K.: 'DC to 40-GHz compact single-layer crossover,' *IEEE Microwave Wireless Comp. Lett.*, 2018, **28**, (8), pp. 642-644.